

Preparation and Properties of Three-Dimensional Ordered Macroporous Loaded Pt-SO₄²⁻/ZrO₂ Solid Super Acid

QIAOWEN CHANG, CAIXIN YAN, JUAN YU, QINGSONG YE, JING JIANG, JIALIN CHEN and WEIPING LIU*

State Key Laboratory of Advanced Technologies for Comprehensive Utilization of Platinum Metals, Kunming Institute of Precious Metals, Kunming 650106, P.R. China

*Corresponding author: E-mail: liuweiping0917@126.com

Received: 4 February 2014;

Accepted: 11 April 2014;

Published online: 15 November 2014;

AJC-16299

Three-dimensional ordered macroporous SiO₂ (3DOMS) was duplicated by using poly(methyl methacrylate) (PMMA) latex spheres as the template. Pt-SO₄²⁻/ZrO₂ solid super acid supported on this macroporous structure material was prepared by impregnation-roasting method and characterized by using TEM, XRD and the N₂ sorption capacity. The effect of ZrO₂ content on the 3DOMS structure was explored. The results indicate that 3DOMS loaded with Pt-SO₄²⁻/ZrO₂ exhibit ordered structure with strong acidity and high BET surface area, when the content for ZrO₂ is optimized to 25 %. The macroporous solid superacid catalysts display high catalytic activity in liquid phase esterification reaction between acetic acid and *n*-butanol.

Keywords: Solid superacid, Three-dimensional ordered macroporous structure, Supported, Pt-SO₄²⁻/ZrO₂, Esterification reaction.

INTRODUCTION

Solid super acids have attracted much attention due to their excellent catalytic activity for isomerization, alkylation and esterification reactions¹. Sulfated oxides, such as sulfated zirconia, titania and iron oxide are common solid super acids and possess high thermostability, super-acidity and high catalytic activity^{2,3}. Most of these catalysts suffer from different drawbacks, particularly low specific surface area and easy deactivation, which can be overcome by the addition of other component and selection of proper support materials. For example, with the addition of Pt element, improved catalytic activity and stability can be achieved⁴⁻⁶. The specific surface area could be largely increased by using ordered porous materials. It was reported that SO₄²⁻/ZrO₂ supported conventional mesoporous materials (MCM-41 or SBA-15) had a high BET surface area⁷⁻¹¹. Unfortunately, the mesoporous structure would be blocked with the increase of loading content of Pt-SO₄²⁻/ZrO₂, a problem that compromises its catalytic activity. A possible solution is to employ macroporous materials as an alternative support. In this context, we report Pt-SO₄²⁻/ZrO₂ supported on three-dimensional ordered macroporous SiO₂ (3DOMS) which shows high catalytic activity in liquid phase esterification reaction between acetic acid and *n*-butanol.

EXPERIMENTAL

Monodisperse poly(methyl methacrylate)(PMMA) spheres were synthesized by a surfactant-free emulsion polymerization

technique according to the literature¹². The poly(methyl methacrylate) spheres were packed into ordered colloidal crystals by centrifugation and dried at room temperature. The molar compositions of the starting precursor (1.0TEOS: 3.51EtOH: 2.27HCl:1.62H₂O) under magnetic stirring formed SiO₂ sol. SiO₂ sol was dropped onto poly(methyl methacrylate) by an impregnated filtration and dried in a vacuum oven at 60 °C for 0.5 h. After repeating the impregnated filtration and drying twice, the composite was calcinated in air at 300 °C for 3 h and then at 600 °C for 4 h, giving rise to the desired three-dimensional ordered macroporous SiO₂ (3DOMS) support.

Pt-SO₄²⁻/ZrO₂ was loaded to 3DOMS by an equal volume impregnation method. ZrOCl·8H₂O in 12 mL ethanol was dropped onto 3DOMS. After dried under 120 °C and roasted under 250 °C for 3 h, the sample was dipped in 0.5 mol/L H₂SO₄ solution for 0.5 h and then dried. Pt-loading was achieved by dipping SO₄²⁻/ZrO₂ on 3DOMS in the acetone solution of Pt(acac)₃ and calcinating at 550 °C for 4 h.

Scanning electron micrographs (SEM) were obtained using a XL30 ESEM-TMP scanning electron microscope. Powder X-ray diffraction (XRD) studies were performed on a Rigaku D/max 2200 diffractometer with CuK_α radiation ($\lambda = 0.15406$) and step-scanned over the 2θ range of 20°-80°, operating at 40 kV and 30 mA. Nitrogen sorption experiments were conducted using a Micromeritics Tristar 3000 automated gas adsorption analyzer. The acid strength of the catalyst was measured by Hammett indicator method.

RESULTS AND DISCUSSION

Closed-packed poly(methyl methacrylate) latex spheres template was prepared by a surfactant-free emulsion polymerization technique. 3DOMS was replicated from the poly(methyl methacrylate) latex spheres template. Fig. 1a is a field emission scanning electron microscopy (SEM) image of the PMMA spheres template. The image shows that the poly(methyl methacrylate) spheres formed 3D ordered array close-packed stacking and the average diameter of the spheres was estimated to be about 320 ± 10 nm. A hexagonal array of the spherical pores, similar to can be clearly observed from SEM of 3DOMS (Fig. 1b), confirming the formation of three-dimensional ordering of the structure. The size of macropore was about 240 ± 10 nm, 25 % smaller than that of the original poly(methyl methacrylate) spheres and average thickness of the walls between the adjacent pores was about 55 nm.

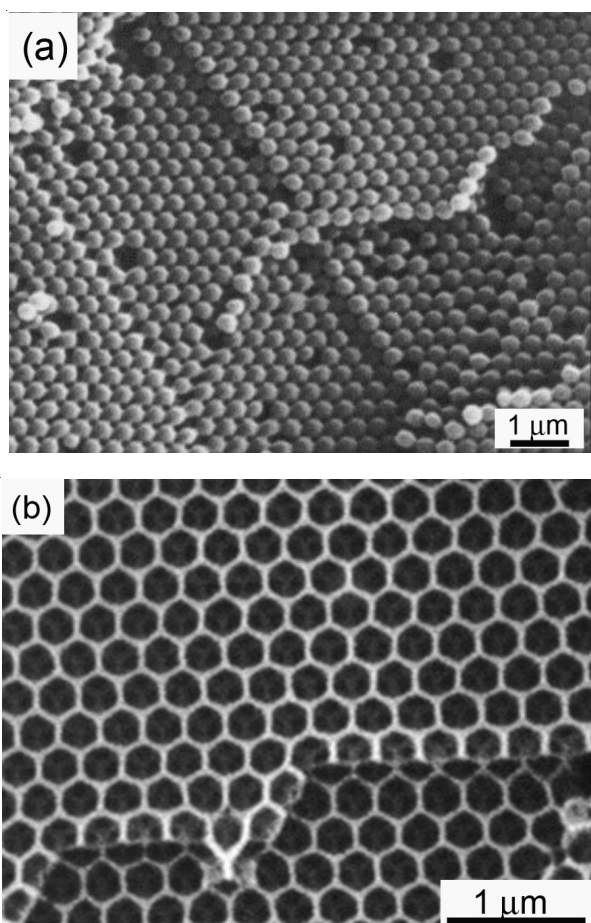


Fig. 1. SEM images of (a) colloidal crystals template assembled from poly(methyl methacrylate) latex spheres and (b) 3DOMS replicated from PMMA template

The SEM images of PSZ/3DOMS with different wt. % of ZrO_2 are shown in Fig. 2. Compared to 3DOMS support, the structure of PSZ/3DOMS was in poor order. The pore diameter increased with the decrease of ZrO_2 content, as illustrated in Table-1. When the ZrO_2 content exceeded 35 %, the particles of ZrO_2 attached onto 3DOMS and the macropores were blocked. Therefore, high ZrO_2 content is unfavorable to the build-up of PSZ/3DOMS.

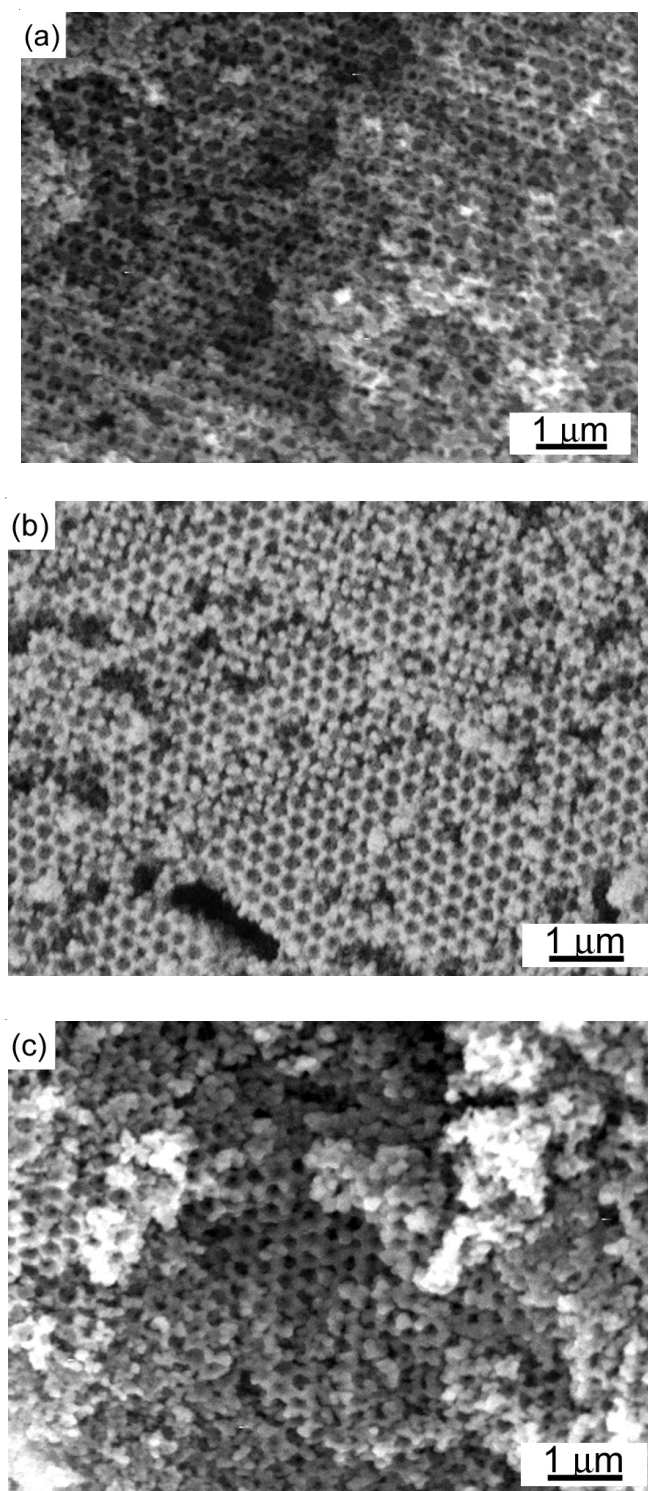


Fig. 2. SEM images of (a) PSZ/3DOMS with different wt. % ZrO_2 (a) 15 %, (b) 25 % and (c) 35 %

TABLE-1
CONTENT OF ZrO_2 AND STRUCTURAL
PARAMETERS OF PSZ/3DOMS SAMPLES

Catalyst	wt. % ZrO_2^*	Porous diameter (nm)	surf. area ($\text{m}^2 \text{g}^{-1}$)
3DOMS	0	240 ± 10	220
PSZ/3DOMS (15 %)	14.5	200 ± 10	196
PSZ/3DOMS (25 %)	23.8	150 ± 5	173
PSZ/3DOMS (35 %)	34.1	120 ± 5	95
Actual ZrO_2 concentration obtained by atomic absorption			

The crystalline structures of PSZ/3DOMS with different ZrO₂ contents were also confirmed by XRD (Fig. 3). The diffraction peaks, due to the four corners of ZrO₂, became stronger with the increase of ZrO₂ content. These peaks are similar to those described in the literature¹². However, diffraction peaks of Pt did not develop, probably because of the low content of Pt (1 %).

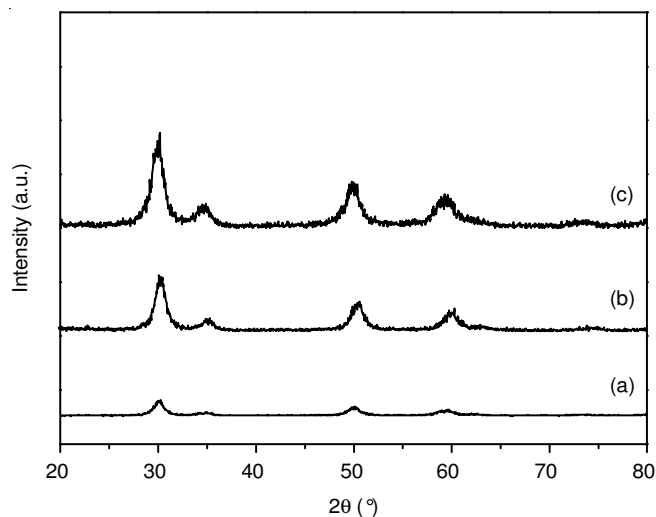


Fig. 3. XRD patterns of (a) PSZ/3DOMS with different wt. % ZrO₂ (b) 15 %, (c) 25 % and 35 %

The pore profiles of the PSZ/3DOMS with wt. % ZrO₂ of 25 % were further characterized by N₂ physisorption (Fig. 4). The shape of the isotherm can be classified as a type II nitrogen adsorption isotherm with a typical macroporous structure. The pore structure parameters with different ZrO₂ contents are given in Table-1.

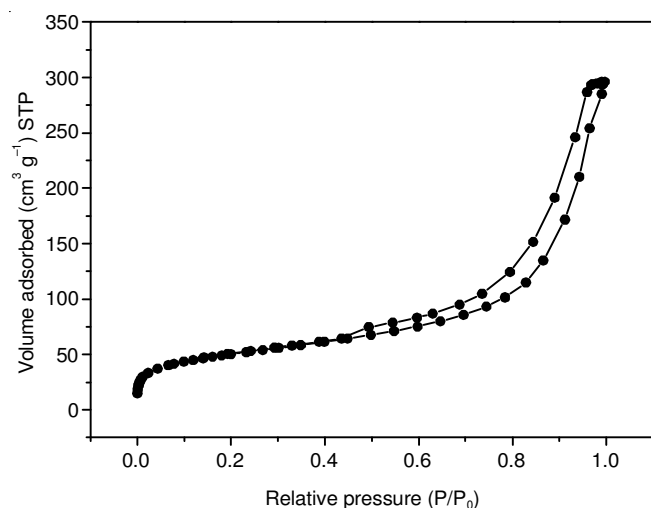


Fig. 4. N₂ Adsorption-desorption isotherm of PSZ/3DOMS with wt. % ZrO₂ of 25 %

The catalytic activities of PSZ/3DOMS with different wt. % ZrO₂ were evaluated in the acetic acid and *n*-butyl alcohol esterification reaction. The related data are listed in Table-2. The conversion rate of CH₃COOH catalyzed by 3DOMS was minimal, only 20 and 56 % by SZ. However, the conversion rate was elevated to 90 % by using 3DOMS as the support when the loading content of ZrO₂ was optimized to 25 % and additional 2 % increase could be achieved by 1 % Pt doping.

TABLE-2
RELATIONSHIP OF COMPOSITION AND STRUCTURE OF CATALYSTS WITH THEIR CATALYTIC ACTIVITIES

Catalysts*	Conversion rate of CH ₃ COOH (%)
SZ	56
3DOMS (0)	20.5
PSZ/3DOMS (15 %)	80.6
PSZ/3DOMS (25 %)	92.7
PSZ/3DOMS (35 %)	75.0
SZ/3DOMS (25 %)	90.6

*Time: 2 h; Temperature: 120 °C

Conclusion

Pt-SO₄²⁻/ZrO₂ supported on 3DOMS, PSZ/3DOMS, was successfully developed in this work. It displayed ordered structure with high BET surface area when the content for ZrO₂ is optimized to 25 %, and catalyzed acetic acid and *n*-butanol esterification reaction in 92.7 % conversion rate.

ACKNOWLEDGEMENTS

The authors are grateful to Yunnan Provincial Science Foundation (Grant No. 2010ZC250, 2012CF003) the National Science Foundation of P. R. China (Grant No. 2013EG115008), for financial support, and Yunnan Tin Group Science Foundation (Grant No. 2012-57A).

REFERENCES

1. M. Hino, S. Kobayashi and K. Arata, *J. Am. Chem. Soc.*, **101**, 6439 (1979).
2. J.C. Yori, J.C. Luy and J.M. Parena, *Appl. Catal. A*, **46**, 103 (1989).
3. R.L. Martins and M. Schmal, *Appl. Catal. A*, **308**, 143 (2006).
4. A. Miyaji, T. Echizen, L.S. Li, T. Suzuki, Y. Yoshinaga and T. Okuhara, *Catal. Today*, **74**, 291 (2002).
5. S. Vijay and E.E. Wolf, *Appl. Catal. A*, **264**, 117 (2004).
6. S. Vijay, E.E. Wolf, J.T. Miller and A.J. Kropf, *Appl. Catal.*, **264**, 125 (2004).
7. Q.H. Xia, K. Hidajat and S. Kawi, *Chem. Commun.*, **5**, 2229 (2000).
8. T. Lei, W.M. Hua, Y. Tang, Y.H. Yue and Z. Gao, *Chem. J. Chin. Univ.*, **21**, 1240 (2000).
9. W. Hua, Y. Yue and Z. Gao, *J. Mol. Catal. A*, **170**, 195 (2001).
10. J. Chen, R. Sun, M. Han, W. Guo and J.T. Wang, *Chin. J. Inorg. Chem.*, **22**, 421 (2006).
11. S. Walspurger and B. Louis, *Appl. Catal. A*, **336**, 109 (2008).
12. J.M. Grau, C.R. Vera and J.M. Parera, *Appl. Catal. A*, **172**, 311 (1998).